A

>hg19_dna range=chr19:5288200-5288799
ACAGGTGCACAAGCCGGTCAAAGTCACACGCAGACACAGGTGCCGGCACACTGTCAGACTATAGATAGGCCAGTCAGTCAGCAGACCACAGGTGCATG<.250
bp.>AGCCTGTGGCCAGCTGGGGCTAGGGTGACCACAGCGGCTGGCCCTGCCCAGAAATGCACATCTGCTTGGCCACACTGAGGGGGCGAGGTCAGTCCCAGACCACTTTGAGCAGCTG
GGCAGGCCTGCAGAGAGCCTCTGGGGAAACTGAGGCAGCATAGCAAACCTGAAGCTCAGAGGGCATGGGTAGGAGTCACTTGCACAGAGAGCCCAGGTGGGGCACATATATGGAGGGCC
CCAGCCACAGCTGGCTCT
>hg19_dna range=chr19:5336300-5336499
ACACTCCACACTCTTGAACCTCAGGGTTAGAGAGACCCAGGTGTCACCTGTTTCCTAGACATTTTGGGGCTGCCACTCTCTGCGTGAGACAACAGCCACCCTTTCCCTCGATCACATCC
CCTACACTTCACTTCCTCTCTCCGTGTCCCCCTTCCTCAATTCAGAATGTCACCTGGTGATAAGATGACATGCATTTGAGC
>hg19_dna range=chr19:5338500-5338811
CGGAAGGCTTTGTGGAGGGCAGCGGGGGGGTAGGGGAGGGATGCCCAGGTGGGGACTCAGTCAGGCCCAAGCTGGGGGGCTGTGGGATTTGAGGGCGGGAAGCAGCCGCCCCCAGCCCC
AGCTGCCTGCCTTCCACCGCCAAAATATCAGCTGGCAAAGAAAGAAGAGCAGAGGGACAGAAGGCAGGCGCGATTGGCAGGGGGAGGGGGGCACAAAGGAAGGGACCCTGGGAGGGGGA
GGGGACTTATGCAAATGGCAGATTCGACCAAGTCCCTGGGCCATTAATAAACGCTCCAGCAGCTGCCGCTGGTA

B

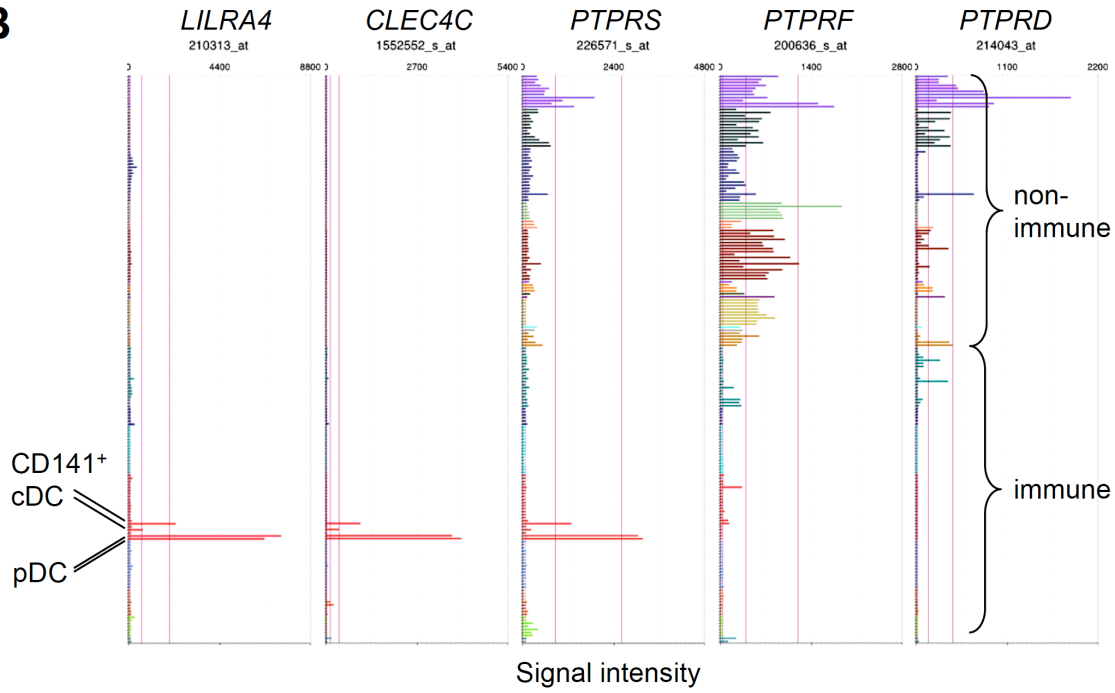

C

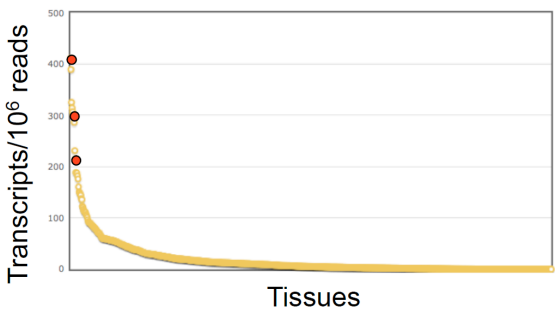

D

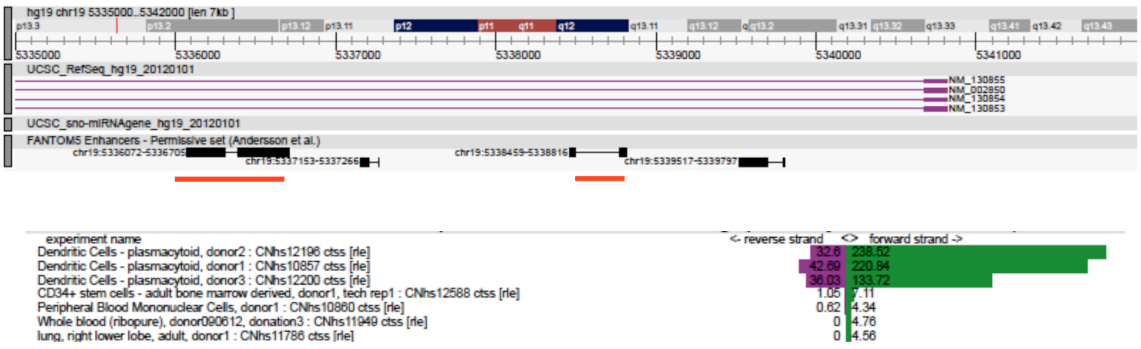

Figure S1 (related to Fig. 1). pDC-specific expression of PTPRS in the human immune system.

(A) Sequences of the the three human genome regions bound by E2-2 within the *PTPRS* locus (Fig. 1A), with the canonical E box sites CAGGTG and CAGCTG highlighted in red and orange, respectively.

(B) Expression profiles of LAR phosphatases in the human primary cell types. Shown are signals of microarray probes for *PTPRS*, *PTPRF* and *PTPRD* across human immune and non-immune cell types in the Primary Cell Atlas dataset (Mabbott et al., 2013) visualized in BioGPS (Wu et al., 2013). Probes for pDC-specific inhibitory receptors BDCA-2 and ILT7 (encoded by *CLEC4C* and *LILRA4*, respectively) are shown for comparison. DC subsets are depicted in red; $CD141^+$ cDC and pDC samples from blood and tonsils (Lindstedt et al., 2005) are indicated.

(C) The expression of the predominant *PTPRS* 5' transcript (p1) across human cells and tissues in the FANTOM5 consortium RNA-Seq database (Forrest et al., 2014). Samples corresponding to primary pDCs are shown in red. All other samples with >100 transcripts per million reads (TPM) correspond to brain tissue.

(D) Enhancers in the first intron of *PTPRS* predicted by the FANTOM5 consortium based on bi-directional transcription activity (Andersson et al., 2014). Shown are the predicted enhancers and the top transcripts derived from them; purple and green indicate sense and antisense transcripts, respectively. Note that nearly all transcripts are derived from pDCs, suggesting a pDC-specific enhancer activity. The regions of E2-2 binding by ChIP-Seq are highlighted in red.

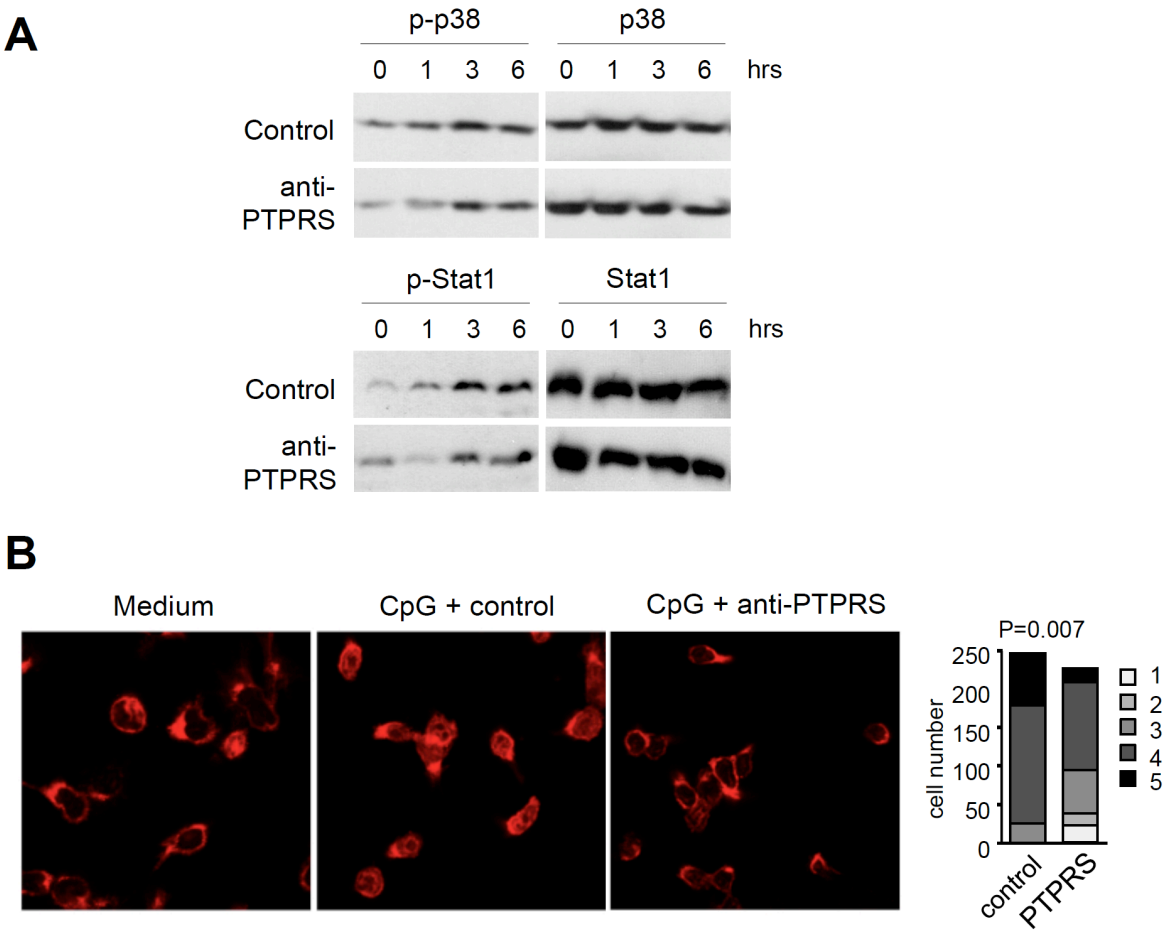

Figure S2 (related to Fig. 3). PTPRS crosslinking inhibits the activation of a pDC cell line

(A) The effect of PTPRS crosslinking on the activation of p38 and Stat1. Gen2.2 cells were activated with CpG for the indicated periods of time in the presence of control or anti-PTPRS antibody, and analyzed by Western blotting for total and phosphorylated p38 and Stat1. Representative of three experiments.

(B) The effect of PTPRS crosslinking on the activation of IRF7. Gen2.2 cells were cultured in medium only or with CpG for 3 hours in the presence of control IgG or anti-PTPRS antibody, fixed, stained for IRF7 and DNA and scored for the degree of IRF7 nuclear translocation. Shown are representative immunofluorescence images of IRF7 staining and the percentage of pDCs with translocated IRF7 on the scale of 1 (full nuclear exclusion) to 5 (homogeneous intracellular staining). Representative of three experiments.

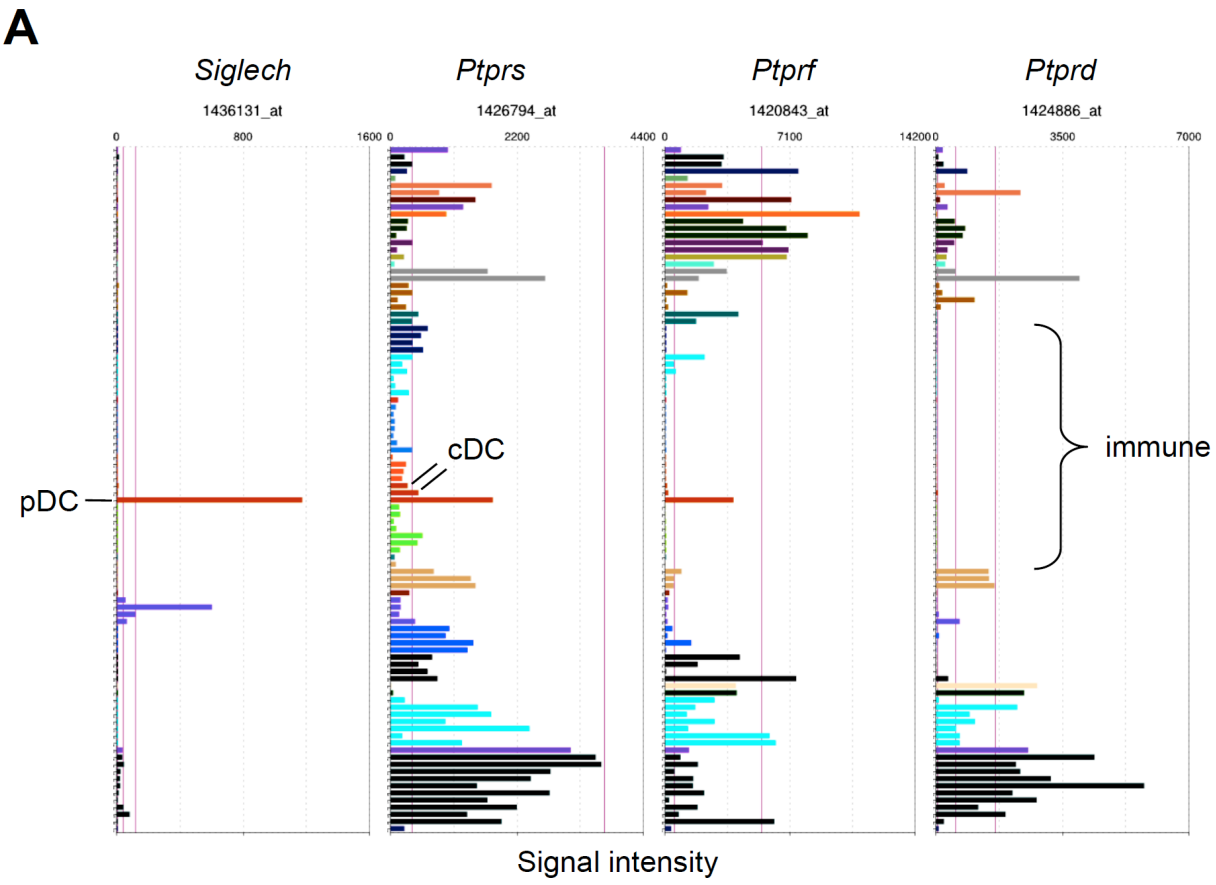

Figure S3 (related to Fig. 4). pDC-specific expression of Ptprs and Ptprf in the murine immune system.

(A) Expression profiles of LAR phosphatases in the murine cells and tissues. Shown are signals of microarray probes for *Ptprs*, *Ptprf* and *Ptprd* across murine immune and non-immune cell/tissue types in the GeneAtlas MOE430 gcrma dataset in BioGPS (Wu et al., 2013). The probes for murine pDC-specific inhibitory receptor SiglecH is shown for comparison. DC subsets are depicted in red; the pDC sample is indicated.

(B) The expression of *Ptprs* and *Ptprf* in E2-2-deficient murine pDCs. Deletion of E2-2 in adult mice was induced by tamoxifen, and splenic pDCs were sorted 5 days later for qRT-PCR analysis (Ghosh et al., 2010). Shown are expression levels relative to the control E2-2-expressing pDC sample (mean ± SD of triplicate reactions).

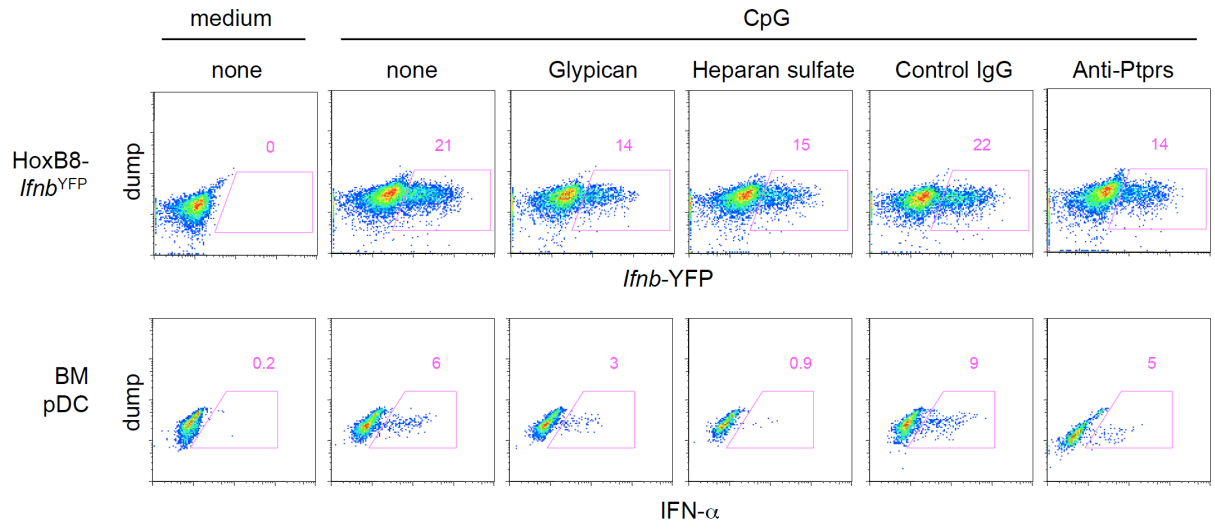

Figure S4 (related to Fig. 5). Inhibitory effect of PTPRS ligands on pDC activation

Cells were incubated with CpG on plates coated with heparan sulfate proteoglycan glypican, heparan sulfate alone, anti-PTPRS antibody or control IgG.

Top row: murine HoxB8-FL cell line carrying the YFP knock-in reporter alleles of *Ifnb* (HoxB8-*Ifnb*^{YFP}) was differentiated into pDCs, activated as above and analyzed for YFP expression 5 hr later. The fraction of YFP^{+} cells is highlighted (representative of three experiments).

Bottom row: total BM cells from wild-type mice were activated as above and stained for pDC markers and intracellular IFN-α. Shown are gated B220^{+} SiglecH^{+} pDCs, with the fraction of IFN-α^{+} cells highlighted (representative of two experiments).

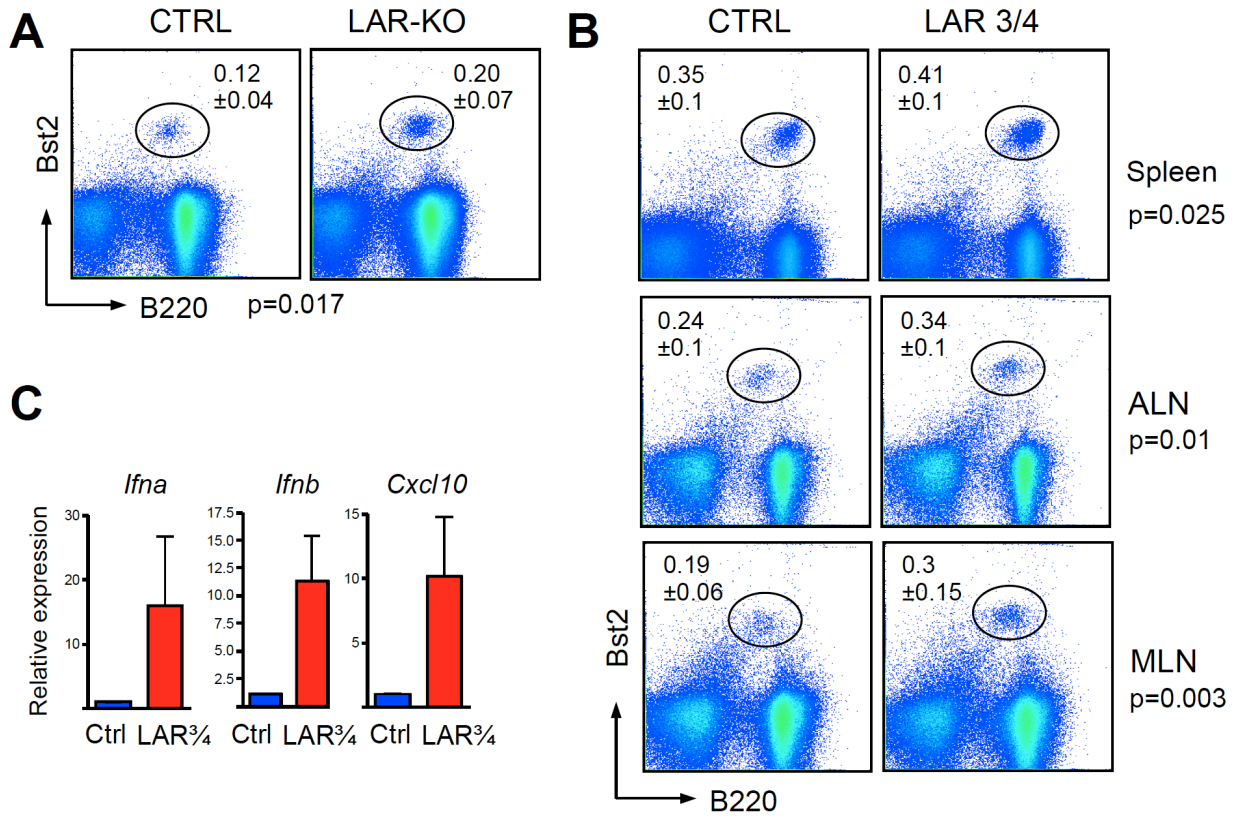

Figure S5 (related to Fig. 6). Characterization of mice with a combined reduction of LAR phosphatases

(A) Splenic pDCs population in mice reconstituted with control or *Ptprs*$^{-/-}$*Ptprf*$^{-/-}$ (LAR-KO) hematopoietic cells. The fraction of B220^{+} Bst2^{+} pDCs is indicated (mean ± SD of 7-10 animals)

(B) The pDCs population in *Ptprs*$^{+/-}$*Ptprf*$^{-/-}$ (LAR3/4) and control mice. The fraction of B220^{+} Bst2^{+} pDCs (mean ± SD) in the spleens (n=22), axillary lymph nodes (ALN, n=12) and mesenteric lymph nodes (MLN, n=20) is indicated.

(C) The expression of IFN genes and IFN-inducible gene *Cxcl10* in the lamina propria lymphocyte preparations of control and LAR3/4 KO mice. Data represent expression levels relative to the control sample as determined by qRT-PCR (mean ± SD of values from 5 individual mice).

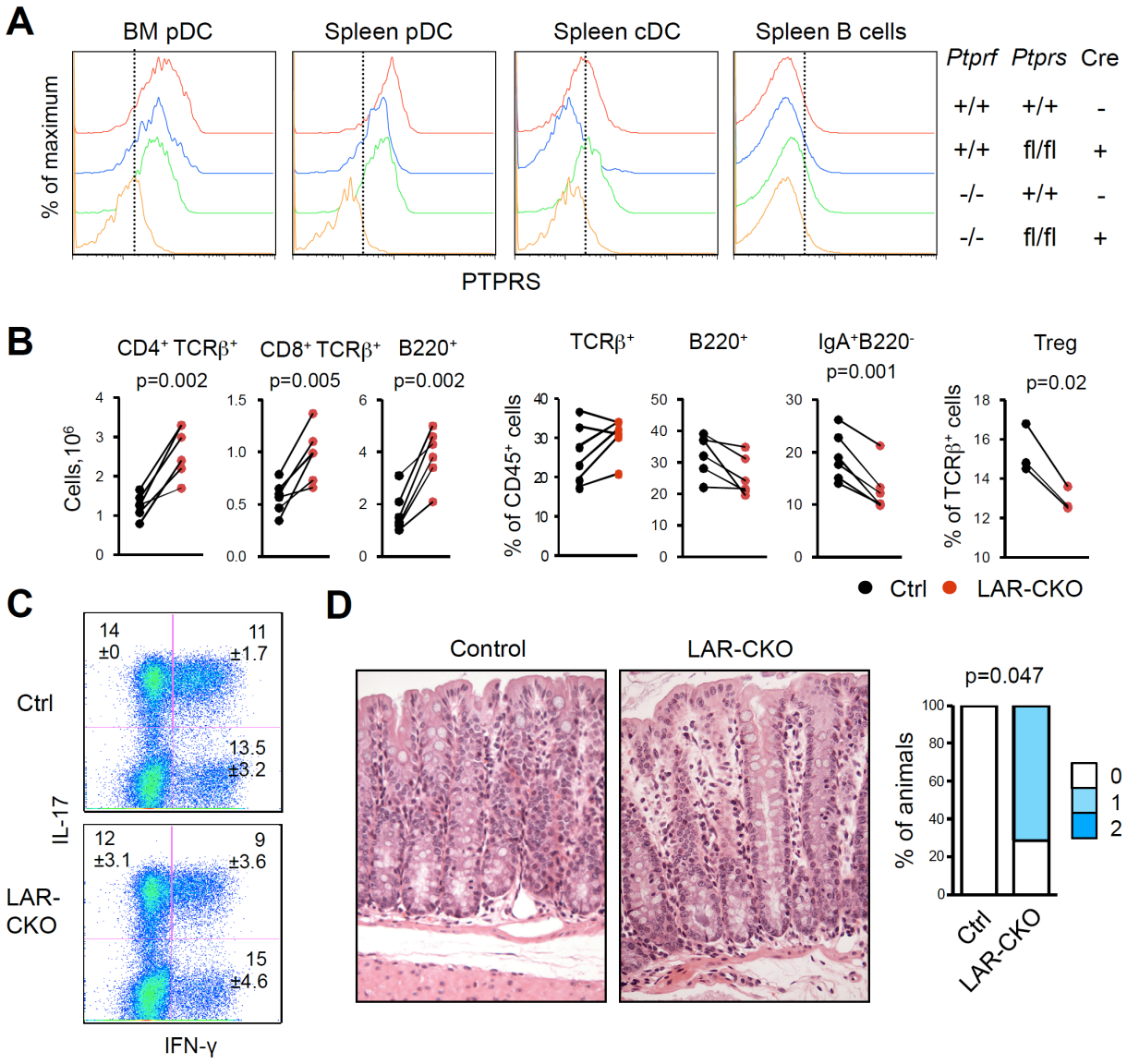

Figure S6 (related to Fig. 7). Characterization of mice with the DC-specific conditional deletion of LAR phosphatases

Animals with conditional LAR phosphatase deletion (LAR-CKO, *Ptprf*$^{-/-}$ *Ptprs*$^{flox/flox}$ *Itgax*^{Cre}) or controls of the indicated genotypes were examined.

(A) Cell surface expression of LAR phosphatases in pDCs from LAR-CKO mice. Total BM cells or splenocytes from mice with the indicated *Ptprs*, *Ptprf* and *CD11c*-Cre genotypes were stained with anti-PTPRS antibodies, followed by secondary fluorescent antibody and antibodies to cell surface markers. Shown are fluorescence histograms in

gated B220^{+} SiglecH^{+} pDCs, CD11c^{hi} MHC II^{+} cDCs and B220^{+} MHC II^{+} SiglecH^{-} B cells; the threshold of positive staining is indicated.

(B) Leukocytes infiltration in the LP of the large intestine. Pairs of LAR-CKO animals and sex-matched littermate controls (*Ptprf*$^{+/-}$ *Ptprs*$^{flox/flox}$ *Itgax*^{Cre}-negative) were co-housed after weaning and analyzed at 2-3 months of age. Shown are absolute numbers of T and B cells; percentages of T and B cells and of IgA^{+} plasma cells; and percentages of FoxP3^{+} CD4^{+} CD25^{+} regulatory T cells out of total TCRβ^{+} T cells. Note that T and B cells in LAR-CKO animals are increased in numbers but not in relative proportions; the proportional decrease of plasma cells likely reflects their local maintenance rather than influx from the blood. Also note the proportional decrease of regulatory T cells, consistent with the ongoing inflammation.

(C) Cytokine production by intestinal LP T cells from LAR-CKO and control animals described above. Total LP lymphocytes from the large intestine were stimulated with PMA and ionomycin and stained for T cell markers and intracellular cytokines. Shown are representative staining plots of gated CD4^{+} T cells, with the fractions of IFNγ^{+} and IL-17^{+} indicated (mean ± SD of values from 3 individual mice).

(D) Representative sections of the large intestines from LAR-CKO mice and *Ptprf*$^{+/+}$ *Ptprs*$^{flox/flox}$ *Itgax*^{Cre}-negative controls (magnification, 200x). The frequency of colitis as scored by histopathology in LAR-CKO (n=7) and control (n=4) mice are also indicated.

Supplemental Materials and Methods

Animals. Wild-type C57BL/6 (B6) mice were purchased from Taconic and maintained in house. *Ptpr*^{GFP} transgenic mice were generated by the GENSAT consortium (Gong et al., 2003) and purchased from the Mutant Mouse Regional Resource Centers repository. Mice with germ-line deletion of *Ptprs* (Elchebly et al., 1999) or *Ptprf* (Schaapveld et al., 1997) were backcrossed onto B6 background for 9 generations and intercrossed (Uetani et al., 2009). Given the defective reproduction and lactation by *Ptprf*-deficient females, *Ptprf*$^{+/-}$ *Ptprs*$^{+/-}$ females were intercrossed with *Ptprf*$^{-/-}$ *Ptprs*$^{+/+}$ or *Ptprf*$^{-/-}$ *Ptprs*$^{+/-}$ males to obtain LAR¾ mice or LAR-KO fetuses, respectively. Because the intercross does not produce wild-type littermates, age-matched wild-type B6 mice that were bred and housed in the same facility were used as controls. For hematopoietic reconstitution, fetal liver cells from LAR-KO or wild-type B6 embryos at 14.5 d.p.c. were transferred into lethally irradiated B6 mice congenic for CD45.1 (B6.SJL, Taconic). Donor reconstitution was >95% in all analyzed chimeras.

The conditional "knockout first" allele of *Ptprs* (*Ptprs*$^{tm1a(KOMP)Mbp}$) in C57BL/6 embryonic stem cells has been generated by the Knockout Mouse Project. Upon blastocyst microinjection and germ line transmission, *Ptprs*$^{tm1a(KOMP)Mbp/+}$ mice were crossed with *Gt(ROSA)26Sor*$^{tm1(FLP1)Dym}$ mice (Jackson Labs) for FLP-mediated excision of the gene trap/selection cassette in the germ line. The resulting mice with the fully conditional *Ptprs*^{flox} allele were outcrossed to remove the FLP allele and crossed to the *Itgax*^{Cre} (Tg(*Itgax*-cre)1-1Reiz/J) strain (Caton et al., 2007) to generate *Ptprs*$^{flox/flox}$ *Itgax*^{Cre} mice with dendritic cell-specific deletion of Ptprs. These mice were then crossed onto *Ptprf*$^{-/-}$ background to generate mice with conditional LAR phosphatase deletion (LAR-CKO, *Ptprf*$^{-/-}$ *Ptprs*$^{flox/flox}$ *Itgax*^{Cre}). Unless indicated otherwise, age-matched *Ptprf*$^{+/+}$ *Ptprs*$^{flox/flox}$ *Itgax*^{Cre}-negative mice from separate breeding cages were used as controls. For the study of colitis in co-housed animals, sex-matched pairs of LAR-CKO mice and littermate *Ptprf*$^{+/-}$ *Ptprs*$^{flox/flox}$ *Itgax*^{Cre}-negative controls were kept in the same cages after weaning.

Human pDC cell lines. Human pDC lymphoma cell lines CAL-1 (Maeda et al., 2005) and Gen2.2 (Chaperot et al., 2006) were cultured in RPMI with 10% FCS; Gen2.2 cells were plated on MS-5 feeder cells. For activation, Gen2.2 cells were plated at

10^6 cells/ml into 24-well plates that were pre-coated with anti-PTPRS or control IgG (1 µg/ml in PBS). CpG type A (ODN 2216, Invivogen) was added 1 hr later at 5 µM concentration, and cells were subsequently lysed for Western blot analysis or fixed for immunofluorescence staining. Western blotting was done using antibodies against PTPRS (Abnova clone 1H6, and R&D Systems #AF3430), and total and phosphorylated p38 and Stat1 (Cell Signaling Technology cat #9212, 9211, 9175, 9171).

For inducible RNAi, CAL-1 and Gen2.2 cells were retrofitted with ecotropic retrovirus receptor and tetracyclin repressor for doxycycline (Dox)-inducible retroviral expression of shRNAs essentially as described (Ngo et al., 2006). Cells were transduced with pRSMX vector-based constructs conferring puromycin resistance and expressing shRNAs under tetracyclin-inducible promoter (Ngo et al., 2006), selected with puromycin and split into parallel cultures with or without 0.5 mg/ml Dox. The shRNA sequences for PTPRS were GGCTTATTCATATTCTGTTCA and CTGTATCCCGTGACATTTCAT. Where indicated, cells were activated with CpG 48 hrs later.

The HoxB8-*Ifnb*^{YFP} cell model. The homozygous *Ifnb*^{YFP} (*Ifnb1*^{tm1Lky}) mice expressing IRES-driven enhanced yellow fluorescent protein (EYFP) from the endogenous *Ifnb1* locus (Scheu et al., 2008) were obtained from Jackson Labs. Total BM cells were transduced with the retrovirus encoding a fusion of HoxB8 and estrogen receptor (HoxB8-ER) and grown in the presence of estrogen and Flt3 ligand (Flt3L)-containing supernatant as described (Redecke et al., 2013). The resulting HoxB8-*Ifnb*^{YFP} cells were cloned by limiting dilution, and a clone with efficient pDC differentiation potential was selected. For pDC differentiation, cells were replated and cultured for 6 days without estrogen in the medium with 10% charcoal-stripped FCS and Flt3L. The resulting cells containing >90% pDCs were replated at $5x10^5$/mL, allowed to settle for 1 hr and stimulated with 1 µM CpG-A for 3-8 hrs.

For Ptprs/Ptprf crosslinking, the plates were pre-coated with goat anti-PTPRS or control IgG (1 µg/ml in PBS). For Fc receptor blockade, 2.5 µg/ml anti-mouse CD16/32 blocking antibody (Fc Block, EBioscience) or 2% goat serum were added to the culture. To immobilize anti-Ptprs antibody via Fc fragments, plates were coated with anti-goat IgG Fc fragment secondary antibody at 10 µg/mL for 1 hr at 37°C, washed and

incubated similarly with anti-PTPRS or control IgG at 4 μg/mL prior to cell plating. For the incubation with PTPRS ligands, plates were first coated for 2 hr at 37°C with poly-L lysine (50 μg/mL) and washed with PBS. The plates were then incubated for 1 hr at 37°C with no ligand, with recombinant mouse glypican 3 or neurocan (R&D Systems), or with heparan sulfate (Sigma) at 10 μg/mL. For tyrosine phosphatase inhibition phosphatase inhibitor cocktail 2 (Sigma) containng sodium orthovanadate was added at the time of plating at a dilution of 1/100. Similar results were obtained with sodium orthovanadate alone.

Intracellular staining. To detect intracellular IFN-α and TNF-α, cells were stained for surface markers, washed and fixed in freshly made 4% paraformaldehyde in PBS for 20 min at room temperature. Cells were washed, permeabilized in PBS with 1% FCS and 0.5% saponin for 10 min and incubated for 30 min with directly conjugated antibodies to IFN-α (PBL Interferon Source, clone RMMA-1) and/or TNF-α (BD Biosciences). Cells were acquired using either BD LSRII or BD Fortessa instruments (BD Biosciences), and data were analyzed using FlowJo software (Treestar). For cell sorting, stained cell suspensions were sorted directly into Trizol LS reagent (Invitrogen) using FACSAria II cell sorter (BD Biosciences).

Immunofluorescence microscopy. Enriched primary human pDCs or Gen2.2 cells were stimulated with CpG with or without control IgG or anti-PTPRS as described above, and transferred onto poly-L-lysine-coated glass slides. Cells were then fixed in 4% paraformaldehyde in PBS for 30 min at room temperature, permeabilized in 0.5% Triton X-100 for 10 min, blocked in CAS-block (Invitrogen) containing 2.5% serum of the same origin as a secondary antibody. Cells were incubated with antibodies against IRF7 or NF-κB p65 subunit (Santa Cruz Biotechnology, sc-9083 and sc-372) or against PTPRS (R&D Systems) in blocking buffer for 1 hr at room temperature, washed and stained with DAPI and with AlexaFluor 647-conjugated anti-rabbit or anti-goat IgG (Invitrogen). Images were acquired using Zeiss LSM 710 confocal microscope and processed by Zen software (Zeiss). The degree of IRF7 and NF-κB nuclear translocation was scored by observers blinded to the identity of the samples.

The analysis of mouse intestinal tissue. The isolation of intraepithelial and lamina propria lymphocytes and stimulation with PMA and ionomycin was done as

described (Ivanov et al., 2006). For histological analysis, intestines were cut longitudinally, rolled by the “Swiss roll” method (Moolenbeek and Ruitenberg, 1981), embedded, sectioned through the central part of the roll and stained with H&E. Stained sections were scored in a genotype-blinded fashion for the evidence of colitis using a composite four-tiered scale (0, normal; 1, mild; 2, moderate; and 3, severe). Detection of CD3 expression by immunohistochemistry on formalin/PFA fixed paraffin embedded sections was performed using a rabbit polyclonal anti-CD3 antibody (ab5690, Abcam). For gene expression analysis of colon tissue, fragments of large intestine measuring 1x1 mm (30-35 mg) were homogenized using Lysing Matrix D beads (MP Biomedical) in RLT buffer supplemented with β-ME from RNeasy kit (Qiagen) using tissue homogenizer (Fast-Prep-24 Instrument, MP Biomedical). RNA was isolated using RNeasy kit according to the manufacturer's instructions.

Supplemental References

Andersson, R., Gebhard, C., Miguel-Escalada, I., Hoof, I., Bornholdt, J., Boyd, M., Chen, Y., Zhao, X., Schmidl, C., Suzuki, T.*, et al.* (2014). An atlas of active enhancers across human cell types and tissues. Nature *507*, 455-461.

Caton, M.L., Smith-Raska, M.R., and Reizis, B. (2007). Notch-RBP-J signaling controls the homeostasis of CD8- dendritic cells in the spleen. J Exp Med *204*, 1653-1664.

Chaperot, L., Blum, A., Manches, O., Lui, G., Angel, J., Molens, J.P., and Plumas, J. (2006). Virus or TLR agonists induce TRAIL-mediated cytotoxic activity of plasmacytoid dendritic cells. J Immunol *176*, 248-255.

Elchebly, M., Wagner, J., Kennedy, T.E., Lanctot, C., Michaliszyn, E., Itie, A., Drouin, J., and Tremblay, M.L. (1999). Neuroendocrine dysplasia in mice lacking protein tyrosine phosphatase sigma. Nat Genet *21*, 330-333.

Forrest, A.R., Kawaji, H., Rehli, M., Baillie, J.K., de Hoon, M.J., Lassmann, T., Itoh, M., Summers, K.M., Suzuki, H., Daub, C.O.*, et al.* (2014). A promoter-level mammalian expression atlas. Nature *507*, 462-470.

Ghosh, H.S., Cisse, B., Bunin, A., Lewis, K.L., and Reizis, B. (2010). Continuous expression of the transcription factor e2-2 maintains the cell fate of mature plasmacytoid dendritic cells. Immunity *33*, 905-916.

Gong, S., Zheng, C., Doughty, M.L., Losos, K., Didkovsky, N., Schambra, U.B., Nowak, N.J., Joyner, A., Leblanc, G., Hatten, M.E., and Heintz, N. (2003). A gene expression atlas of the central nervous system based on bacterial artificial chromosomes. Nature *425*, 917-925.

Ivanov, II, McKenzie, B.S., Zhou, L., Tadokoro, C.E., Lepelley, A., Lafaille, J.J., Cua, D.J., and Littman, D.R. (2006). The orphan nuclear receptor RORgammat directs the differentiation program of proinflammatory IL-17+ T helper cells. Cell *126*, 1121-1133.

Lindstedt, M., Lundberg, K., and Borrebaeck, C.A. (2005). Gene family clustering identifies functionally associated subsets of human in vivo blood and tonsillar dendritic cells. J Immunol *175*, 4839-4846.

Mabbott, N.A., Baillie, J.K., Brown, H., Freeman, T.C., and Hume, D.A. (2013). An expression atlas of human primary cells: inference of gene function from coexpression networks. BMC Genomics *14*, 632.

Maeda, T., Murata, K., Fukushima, T., Sugahara, K., Tsuruda, K., Anami, M., Onimaru, Y., Tsukasaki, K., Tomonaga, M., Moriuchi, R.*, et al.* (2005). A novel plasmacytoid dendritic cell line, CAL-1, established from a patient with blastic natural killer cell lymphoma. Int J Hematol *81*, 148-154.

Moolenbeek, C., and Ruitenberg, E.J. (1981). The "Swiss roll": a simple technique for histological studies of the rodent intestine. Lab Anim *15*, 57-59.

Ngo, V.N., Davis, R.E., Lamy, L., Yu, X., Zhao, H., Lenz, G., Lam, L.T., Dave, S., Yang, L., Powell, J., and Staudt, L.M. (2006). A loss-of-function RNA interference screen for molecular targets in cancer. Nature *441*, 106-110.

Redecke, V., Wu, R., Zhou, J., Finkelstein, D., Chaturvedi, V., High, A.A., and Hacker, H. (2013). Hematopoietic progenitor cell lines with myeloid and lymphoid potential. Nat Methods *10*, 795-803.

Schaapveld, R.Q., Schepens, J.T., Robinson, G.W., Attema, J., Oerlemans, F.T., Fransen, J.A., Streuli, M., Wieringa, B., Hennighausen, L., and Hendriks, W.J. (1997). Impaired mammary gland development and function in mice lacking LAR receptor-like tyrosine phosphatase activity. Dev Biol *188*, 134-146.

Scheu, S., Dresing, P., and Locksley, R.M. (2008). Visualization of IFNbeta production by plasmacytoid versus conventional dendritic cells under specific stimulation conditions in vivo. Proc Natl Acad Sci U S A *105*, 20416-20421.

Uetani, N., Bertozzi, K., Chagnon, M.J., Hendriks, W., Tremblay, M.L., and Bouchard, M. (2009). Maturation of ureter-bladder connection in mice is controlled by LAR family receptor protein tyrosine phosphatases. J Clin Invest *119*, 924-935.

Wu, C., Macleod, I., and Su, A.I. (2013). BioGPS and MyGene.info: organizing online, gene-centric information. Nucleic Acids Res *41*, D561-565.